J. W. Lynn
NCNR

Choice of Spectrometer for Inelastic Scattering

I. General Considerations

At the NCNR we have several types of spectrometers that are designed to measure excitations in materials. The instruments that you will be using in the workshop are the cold neutron triple-axis instrument (SPINS), the filter analyzer spectrometer (FANS), the backscattering spectrometer (HFBS), the disk chopper time-of-flight spectrometer (DCS), and the spin-echo spectrometer, but in our discussions here we will also include the thermal triple-axis instruments along with the Fermi chopper spectrometer so that you will have a complete overview of the inelastic instrumentation available at the NCNR. Each of these spectrometers has an energy range E and related wave-vector range $\boldsymbol{Q}$ over which it can measure excitations, with an associated energy resolution and wave-vector resolution. The choice of spectrometer is determined by how these capabilities match the excitations of interest. Therefore to make a choice you need to have an idea both of the type of excitation(s) of interest (for example molecular vibrations, phonons, magnons, diffusion, crystal field excitations) and the overall scale of the energetics. Often it is necessary to collect data on more than one spectrometer in order to cover the complete energy range of the excitations.

In this section we discuss the basics of these instruments, and the best place to start is with the energy-momentum relationship for the neutron. The energy of a neutron is related to the momentum $p = \hbar k$ by

$$E_{neutron} = \left(\frac{p^2}{2m}\right) = \left(\frac{\hbar^2 k^2}{2m}\right) = 2.072138 k^2 = \left(\frac{h^2}{2m\lambda^2}\right) = 81.8047/\lambda^2 \qquad (1)$$

where the magnitude of the wave vector $k = 2\pi/\lambda$ is in $Å^{-1}$ and the wavelength λ is in Å. The energy is in meV.

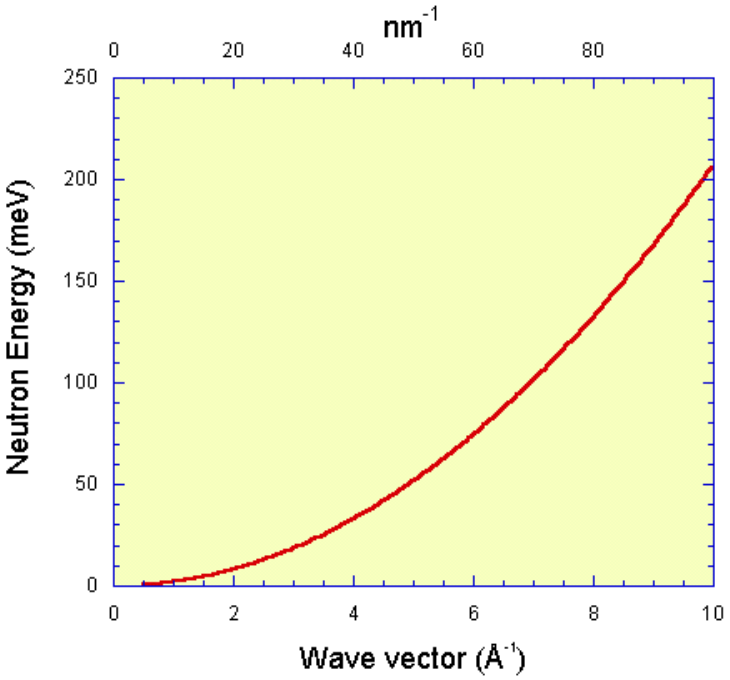

Fig. 1. Dispersion relation for the neutron.

One of the fundamental characteristics of neutrons is that for wavelengths comparable to interatomic spacings, the neutron energy is of the same order as the energy of thermal excitations k_BT (k_B is Boltzmann's constant) in materials, and this makes it straightforward and convenient to determine the changes of energy that occur upon scattering. In particular, the conversion between energy and temperature is

$$1\,meV = 11.60457\,K \quad . \qquad (2)$$

Room temperature (~295 K) then corresponds to an energy of about 25 meV, which for a neutron corresponds to a wavelength of 1.8 Å.

For comparison with other types of measurements, we note that other experimental techniques have adopted specific units to indicate the energy of excitations. Raman scattering and infrared absorption, for example, use wave numbers, where $1\,meV = 8.06549\,cm^{-1}$. For vibrations (such as phonon energies), frequency is often used, and $1\,meV = 0.24180\,THz$. Finally, neutron scattering is used to investigate magnetic ordering and spin dynamics in magnetic systems, and in this case a 1 μ_B magnetic moment in an applied field of 17.2766 Tesla corresponds to an energy of 1 meV ($1\,meV / \mu_B = 17.2766\,T$).

It is also instructive to compare these neutron characteristics with other scattering probes such as x-rays and electrons. For photons the dispersion relation is

$$E_{photon}(keV) = 1.97328k = 12.3985/\lambda \qquad (3)$$

while for electrons we have

$$E_{electron}(eV) = 3.81000k^2 = 150.413/\lambda^2 \quad . \qquad (4)$$

A familiar example is the characteristic k_α x-ray radiation for Cu, which has a wavelength of 1.54 Å and thus an energy of 8.05 keV. This energy corresponds to a temperature of $9.3 \cdot 10^7$ K. For an electron of this same wavelength the energy is 63.4 eV, which is equivalent to a temperature of $7.4 \cdot 10^5$ K. For a neutron with this wavelength the energy is 34.5 meV, corresponding to 400 K, which is just in the energy range of excitations that are typically populated thermally. It is fortuitous that the energy-momentum relation for neutrons provides them with a clear advantage when measuring excitations in materials.

II. The scattering of a neutron

A neutron incident on a sample with wave vector $\mathbf{k}_i$ and energy E_i is scattered into a final wave vector $\mathbf{k}_f$ and final energy E_f. The total momentum and energy must be conserved in the scattering process, and thus there must be a corresponding change in the crystal momentum and energy. The changes in wave vector **Q** and energy ΔE can be written as

$$\mathbf{Q} = \mathbf{k}_i - \mathbf{k}_f \qquad (5)$$

and

$$\Delta E = \frac{\hbar^2 k_i^2}{2m} - \frac{\hbar^2 k_f^2}{2m} \qquad (6)$$

respectively. This is conveniently represented in a scattering diagram

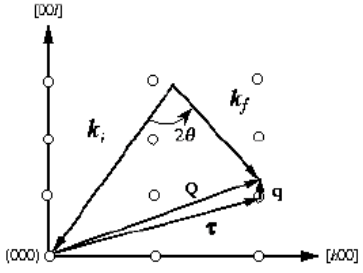

Fig. 2. Scattering diagram of Reciprocal Space. Note that in these diagrams **Q** can refer (usually interchangeably) to the change in neutron wave vector, or the wave vector of the excitation in the crystal.

where the open circles represent the positions of Bragg peaks in a single crystal. For this particular example the single crystal is oriented in the scattering plane defined by the [*h,0,0*] and the *[0,0,l*] vectors, in other words, the [*h,0,l*] scattering plane. The wave vector **Q** can be written as

$$\mathbf{Q} = \tau + \mathbf{q} \tag{7}$$

where $\boldsymbol{\tau}$ is the reciprocal lattice vector and **q** is the (periodic) reduced wave vector for the elementary excitation being measured. The angle labeled 2θ is the scattering angle defined by the change in direction of the neutron from $\mathbf{k}_i$ and $\mathbf{k}_f$, while the orientation of $\mathbf{k}_i$ can be changed by a simple rotation of the sample. In this example we have $k_i > k_f$, so the neutron loses energy in this scattering process (termed energy loss) while creating an excitation in the sample; energy gain is when $k_i < k_f$, and an excitation is destroyed in the sample. By experimentally varying both **Q** and the energy transfer, the dynamics in the system of interest can be explored over a wide range of wave vectors. There are some restrictions, however, that are imposed by the conservation conditions (Eqs. (5) and (6)). The wave vector transferred can certainly be no larger than $k_I + k_f$ (2θ= 180º), and typically this is restricted to angles considerably smaller than this (e.g. ~120º). The energy loss spectrum also is restricted to energies below E_i. At small wave vectors, on the other hand, the dynamical range is quite restrictive as shown in Fig. 3. For a fixed magnitude of the wave vector **q**, the largest possible difference in energies is achieved when $\boldsymbol{k_I}$, $\boldsymbol{k_f}$ and **q** are all collinear, where we then have that k_I =q+ k_f (energy loss) or k_I + q = k_f (energy gain). In practice this condition requires that 2θ=0º, which means that the analyzer system is looking directly into the incident beam. Hence the practical range of energy transfers is restricted even further.

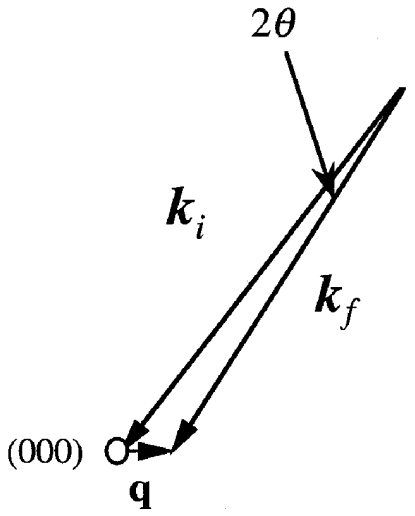

Fig. 3. Small **q** scattering diagram

The reciprocal lattice shown schematically in Fig. 2 is quite simple, where each reciprocal lattice vector is given by

$$\tau(h,0,l) = \left(h\frac{2\pi}{a}, 0, l\frac{2\pi}{c} \right) \tag{8}$$

and *a* and *c* are the real-space lattice parameters. If the sample is polycrystalline in nature, the basic neutron scattering diagram is the same, but the reciprocal lattice of the ensemble of crystals takes on all possible orientations. Each reciprocal lattice point can be thought of as sweeping out a sphere of radius τ, and the scattering plane then cuts these spheres to produce circles as shown in Fig. 4.

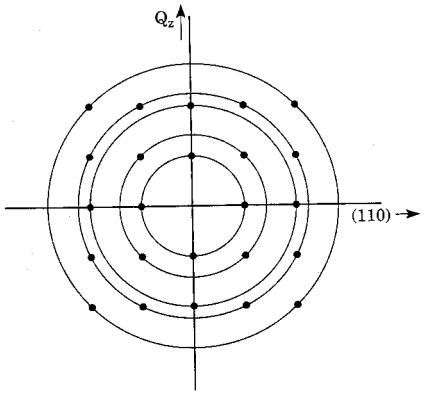

Fig. 4. Reciprocal space of a crystal (solid points) and for a powder sample (rings).

For a polycrystalline sample it is then not possible to make the decomposition indicated in Eq. (7), and therefore the reduced wave vector of any observed excitation cannot be determined. Rather, the density of states of the excitations is measured, which can then be compared with other related materials, with other spectroscopic techniques, and with theoretical models of the excitations of the system.

III. Crystal Spectrometers

Triple-axis instrument

The triple-axis spectrometer is perhaps the simplest of the inelastic instruments conceptually. The first axis is for the monochromator crystal, which defines the incident neutron wavelength via Bragg's law:

$$\lambda_i = 2d_M \sin(\theta_M) \qquad (9)$$

where d_M is the crystallographic *d* spacing for the monochromator crystal. The neutron wavelength is then selected by changing the diffraction angle θ_M (labeled #1 in Fig. 5) as well as the monochromator shielding "drum" angle $2\theta_M$, labeled #2 in Fig. 5. The second axis contains the sample orientation (#3) and the sample scattering angle (#4) 2θ (also see Fig. 2). The third axis then consists of an analyzer (#5) crystal and detector angle (#6) to specify the scattered energy, again via Bragg's law:

$$\lambda_f = 2d_A \sin(\theta_A) \quad . \qquad (10)$$

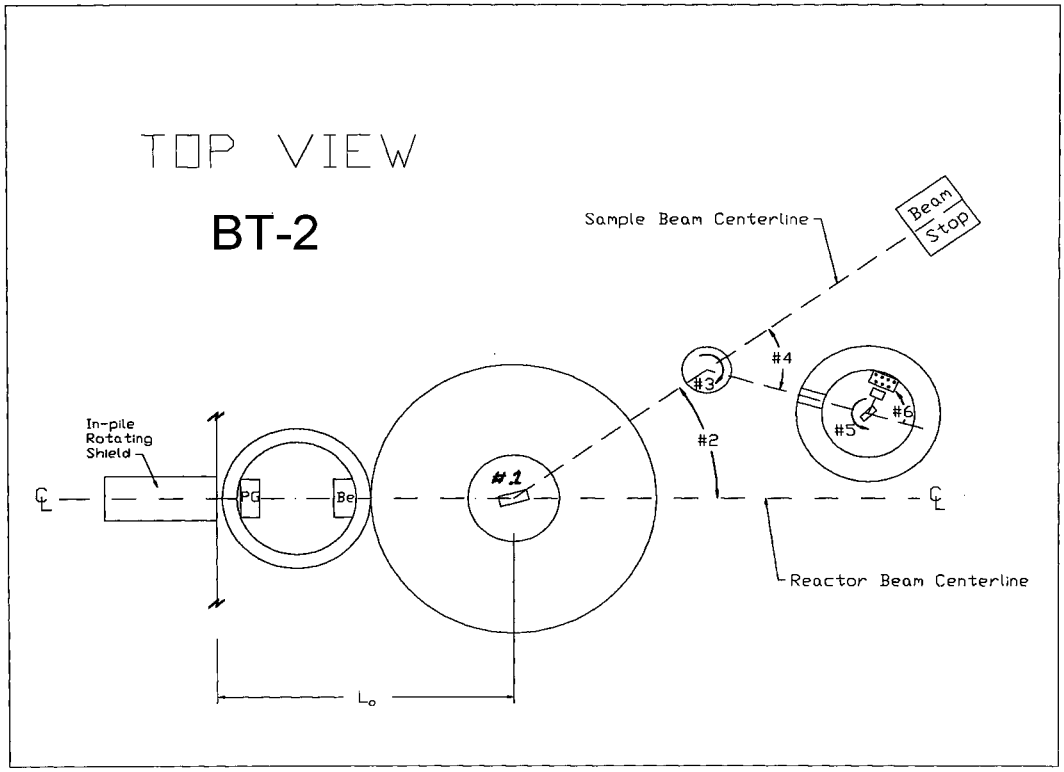

Fig. 5. BT-2 thermal triple-axis spectrometer.

This defines the incident and scattered neutron wave vectors and energies, and these can be varied in a continuous manner by varying the angles of the three axes, to map out the dispersion relations for the excitations.

An essential characteristic of an instrument is the dynamical range that the instrument is capable of providing. All five triple-axis instruments (BT-2, BT-4, BT-7, BT-9, and SPINS) have (among others) a pyrolytic graphite monochromator (d_M =3.35416 Å), and the range of angle #2 then determines the range of incident energies available. For BT-2 this angular range determines the incident energy range to be between 55 meV and 4.9 meV, while for SPINS the energy range is from 2.2 meV to 14 meV. This gives a useful energy transfer of from 0 (elastic scattering) to ~50 meV for BT-2, and 0-12 meV for SPINS.

A second important characteristic is the energy resolution of the spectrometer. If we take the derivative of Eq. (9) we have

$$\Delta\lambda = 2d_M \cos(\theta_M)\Delta\theta_M \qquad (11)$$

and we see that the wavelength spread is related to the angular resolution before and after the monochromator, and this is under the control of the experiment. A similar spread occurs for the analyzer. In terms of energy we have

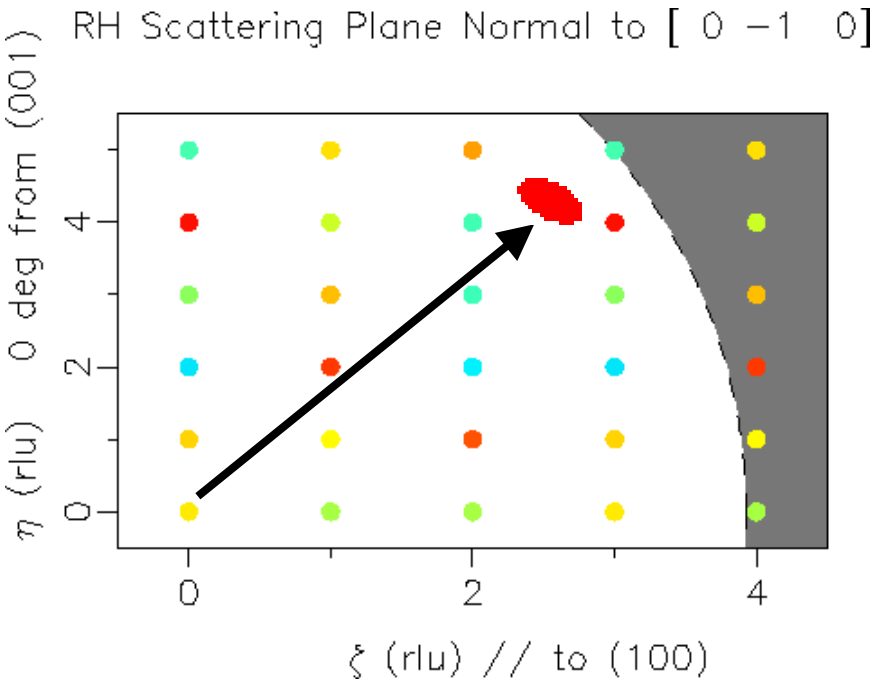

Fig. 6. Example of reciprocal space for thermal neutrons (35 meV), with the instrumental resolution depicted. The dark region indicates scattering angles that are too large for the instrument, and are hence inaccessible.

$$\Delta E_{\mathrm{Res}} \propto \left(\frac{h^2}{m\lambda^3} \right) \quad . \tag{12}$$

Looking at the scattering diagram in Fig. 2, we see that spreads in wavelength and angle contribute not only to the energy resolution, but they also give rise to a spread in wave vectors that contributes to the Q resolution as indicated in Fig. 6. The resolution can be improved by decreasing the angular collimations of the instrument, with a concomitant decrease in the neutron flux on the sample, and into the detector. However, Eq. (12) indicates that the most effective way to improve the energy resolution is to use longer wavelength neutrons, but again with a corresponding decrease in flux. This brings us into the realm of cold neutrons, and a general paradigm is that cold neutrons are synonymous with high resolution. The use of long wavelength neutrons, though, restricts the range of accessible wave vectors as indicated in Fig. 7. Here we have drawn the same reciprocal space as shown in Fig. 6 for thermal neutrons, but now we are employing cold neutrons with an incident energy of 3.5 meV.

We see that there are three basic factors that determine the appropriate instrument for your measurements, and although we have been discussing the triple-axis spectrometer, these general deductions apply equally well to all the inelastic instruments. The first factor is the energy of the excitations; high

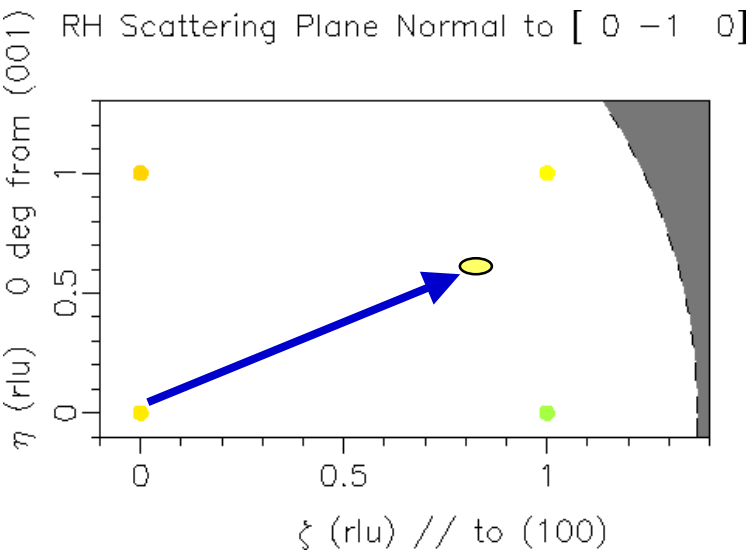

Fig. 7. Reciprocal space for cold neutrons.

energy excitations generally can be best measured with thermal neutrons, while cold neutrons are best suited for low energy excitations. The second factor is the wave vector dependence of the excitations. For example, the scattering intensity for lattice vibrations has an overall factor $\propto Q^2$, as well as energies that go up to the 50-100 meV range or higher, and hence these types of excitations are usually measured with thermal neutrons. Acoustic phonons and soft phonons, in contrast, have energies that extend to zero energy, so the thermal measurements often are complemented with cold neutron data (and we'll see some examples below). Magnetic scattering, on the other hand, contains a magnetic form factor in the cross section which is large at small Q and typically drops off relatively quickly with increasing Q, so that cold neutrons are often ideal for magnetic studies (if the excitation energies are not too high). The final consideration is the instrumental resolution that is needed/desired for the measurements, and generally cold neutron instrumentation provides better resolution.

If you think that these requirements appear to be in conflict with one another, you are exactly correct. Every neutron experimenter would like to have more intensity, larger dynamical range, and higher resolution; it is up to the experimenter to balance these conflicting requirements and obtain the best data possible.

Backscattering Spectrometer (HFBS)

The energy resolution of a thermal triple-axis spectrometer depends on the incident energy and monochromator/analyzer *d*-spacings as just discussed qualitatively, but a figure of merit is that the resolution is ~1 meV (using pyrolytic graphite). If we need better resolution a cold triple axis can be employed, and the

figure of merit for resolution is ~0.1 meV, or 100 μeV. If still better energy resolution is needed, then Eq. (10) suggests perfect resolution ($\Delta\lambda \equiv 0$) can be achieved in the backscattering condition ($\theta_M = 90°$; $2\theta_M = 180°$). In practice the resolution that can be achieved is ~1 μeV, approximately two orders of magnitude better than on a cold triple-axis instrument. The condition that $\Delta\lambda \approx 0$, however, means that the flux onto the sample will be severely reduced, and thus the angular divergences need to be relaxed in order to obtain sufficient signal. To achieve these conditions requires a completely different instrument design and construction--hence the High Flux Backscattering Spectrometer. Furthermore, the energy cannot be varied by changing the monochromator/analyzer angle as for a conventional triple axis since we already are at the backscattering condition. Rather, the incident energy is varied by physically moving the monochromator at a speed v with respect to the sample, and thereby changing the energy incident on the sample. This is an identical technique to that used in Mössbauer spectroscopy. This Doppler shifting provides a dynamical range as high as ±40 μeV, and of course the Q-dependence of the scattering can be determined. The details of this spectrometer are quite different from a thermal or cold triple-axis instrument, but the basic concept is the same.

Filter Analyzer Neutron Spectrometer (FANS)

The basic design of the filter analyzer spectrometer is again a triple-axis instrument, but the crystal analyzer is replaced by a filter analyzer (as the name implies). This energy-analyzer consists of a thick (15 cm) block of polycrystalline Be, followed by a 15 cm block of polycrystalline graphite. The idea is that for every crystalline system there are Bragg powder lines (as indicated in Fig. 4, for example), and a neutron traveling through the material will find a crystallite oriented at the Bragg angle, and scatter. The probability for transmission directly through the material is then very low. There is a set of reciprocal lattice vectors that is closest to the origin, however, and if the neutron wavelength is too long (i.e. $k_i = k_f$ is small enough) then there is no possibility of satisfying the Bragg scattering for any orientation of $\boldsymbol{k}_i$. and $\boldsymbol{k}_i$; $\boldsymbol{Q}$ in Eq. (5) is simply not long enough to reach the first reciprocal lattice vector. The materials are chosen to have negligible absorption cross sections, and with the Bragg scattering eliminated the only significant scattering process that can occur is inelastic (phonon) scattering. To reduce this possibility, the whole analyzer system is cooled to liquid nitrogen temperatures. The neutrons beyond the Bragg cutoff will then be transmitted with high probability. For the Be/PG combination the Bragg cutoff occurs at a wavelength of 6.7 Å (energies below 1.8 meV). Taking into account this transmission, detector efficiency, etc. the average scattered energy is ~1.1 meV (well into the cold neutron regime).

The monochromator portion of the spectrometer is in fact a triple-axis spectrometer, with a choice of either pyrolytic graphite, or Cu(220) (d=1.27 Å) which provides incident energies up to 200 meV. The basic scattering diagram then looks like Fig. 8, where we see that the scattering wave vector is

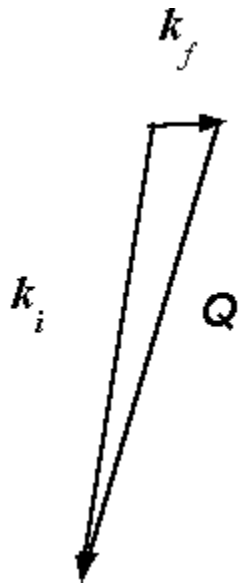

Fig. 8. Typical scattering diagram for FANS

approximately $\boldsymbol{k}_i$, and the incident energy is approximately the energy of the excitations measured. The sample is typically a polycrystalline material, but glasses and fluids can also be measured, and the instrument is capable of directly determining the density of states for lattice vibrational excitations over the energy range from ~20 meV to 200 meV.

Spin Echo Spectrometer

The overall layout of the spin-echo spectrometer is similar to the spectrometers already discussed, but the functioning of the instrument is completely different. We start with incident neutrons, which are selected by a velocity selector for a wavelength between 5 and 15 Å, but with a very large spread in wavelengths, $\Delta\lambda$~15%. The direction of $\boldsymbol{k}_f$ relative to $\boldsymbol{k}_i$. is varied in the same way as a conventional triple-axis instrument, while the analyzer is a polarizing supermirror and detector, which again has very coarse wavelength selection. The conventional part of the instrument therefore does not provide useful energy resolution. However, the concept of spin echo is that the energy resolution is not tied to the wavelength of the neutrons at all, but rather to the Larmor precessional frequency of the magnetic moment of the (polarized) neutrons as they pass through the instrument, in a magnetic field. This technique in fact has the capability of providing the best energy/time resolution of any neutron scattering spectrometer.

The concept of spin echo is straightforward in principle. We polarize the incident neutrons so their spins all point in the same direction, which is along the direction of their motion. Then as they approach the sample, we rotate the polarization so that it is perpendicular to the magnetic field. The spin then

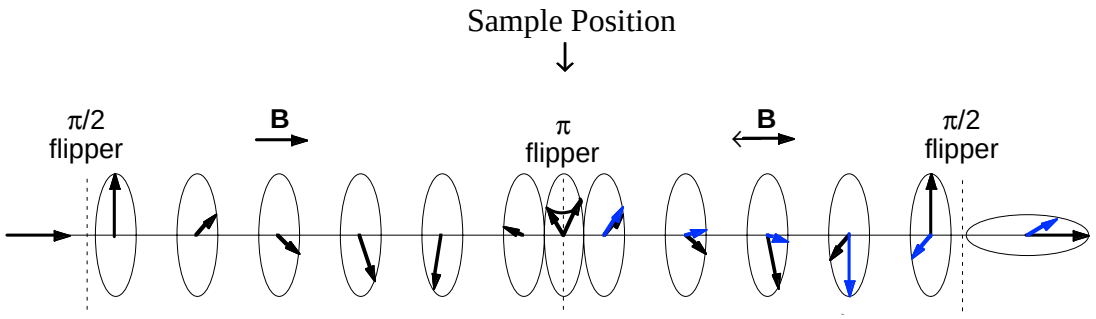

Fig. 9. Larmor precession of the neutron spin. Before the sample the precession is clockwise as view from the detector, while after it is in the opposite sense.

precesses with angular frequency $\omega=\gamma B$, where γ is the gyromagnetic ratio of the neutron. If the speed of the neutron is v and the distance to the sample is *L*, the time it takes for the neutron to get to the sample is

$$t = \frac{L}{\mathrm{v}} \quad . \tag{13}$$

The neutron spin will then have precessed by an angle

$$\phi = \omega t = \frac{\gamma B L}{\mathrm{v}} \quad . \tag{14}$$

At the sample position, the spin of the neutron is flipped by 180°, and it causes it to precess in the opposite sense. If we take the simple case of equal path lengths and equal magnetic fields before and after the sample, then it is easy to see that the neutron spin will "wrap-up" on the way to the sample with a phase angle φ, and then "unwrap" on the way to the detector with a phase angle $-\varphi$, as indicated in Fig. 9. This yields no change in the phase angle of the neutron spin. It should be noted that if the next neutron has a different speed (which it certainly will with a $\Delta\lambda\sim15\%$), then the precession angle φ' will be different when it arrives at the sample, but then it will "unwrap" by exactly $-\varphi'$ on the way to the detector. This is the echo condition. This technique allows a broad wavelength distribution of neutrons to be used, greatly enhancing the flux, while maintaining the very high sensitivity in measuring the change in energy of the neutron.

If the neutron gains a little energy at the sample, it will get to the detector a little bit sooner, and we will see this as a small decrease in phase angle, and consequent change in the detected polarization. Alternatively, if the neutron loses a little energy it will arrive at the detector system a little later, and the phase angle will have increased compared to the elastic (no change in speed) case. Eq. (13) indicates that these changes in the polarization are related to the time, and we can change this time by varying the magnetic field along the paths before and after the

sample, while maintaining the echo condition. Thus data are actually collected on a spin-echo spectrometer by sweeping the spin-echo field of the spectrometer, thereby obtaining the time-dependence of the scattering intensity as a function of **Q**. In terms of the cross sections, we determine the intermediate scattering function I(**Q**,t), rather than the scattering function S(**Q**,ω) as on a conventional spectrometer. Hence we are actually making a different kind of measurement. We can obtain an estimate for the effective energy resolution, however, by using the Heisenberg uncertainty relation ($\Delta t \cdot \Delta E \approx \hbar$), and find that the spectrometer has a resolution capability of ~50 neV.

Disk Chopper Spectrometer (DCS)

An alternate way to measure inelastic scattering is by time-of-flight. The basic principle is to send a short burst of monochromatic neutrons onto the sample, and then measure the time of arrival at a series of detectors that cover a wide angular range; in the case of DCS there are over 900 detectors. If the neutrons are elastically scattered they arrive at time t_0, while if they gain some energy from the sample they arrive earlier, and if they lose energy they arrive later. We then measure the time distribution of neutrons arriving at each detector, and relate this directly to the change in energy to determine the scattering function S(**Q**,ω). After all the neutrons have been collected, we send another pulse of monochromatic neutrons and repeat the measurement. We want this repetition rate to be as short as practical in order to make the best use of the neutrons available from the reactor, while having the pulses far enough apart in time that we don't confuse slow energy-loss neutrons from one pulse with fast energy-gain neutrons from the next pulse (called frame overlap).

Figure 10 shows the scattering diagram for a single detector of a time-of-flight spectrometer; the detector is stationary, at a fixed scattering angle. The elastic condition is when $k_I = k_f$, is shown by the red dotted vectors, two energy loss processes by the blue dotted and black solid vectors. The neutron arrival

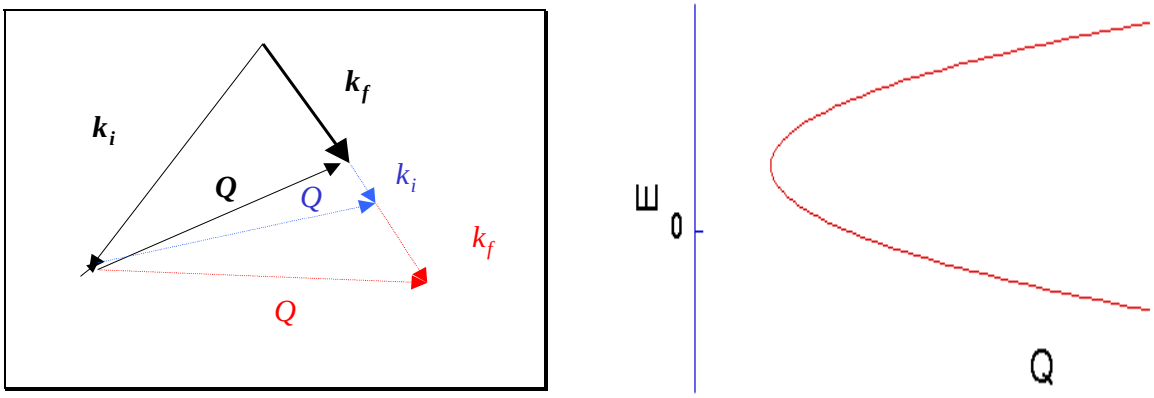

Fig. 10. (left) The scattering diagram for a single detector. (right) trajectory in (E, Q), where Q is the magnitude of the wave-vector transfer.

time can be determine accurately, and typically there are ~10^3 time channels of data so that the distribution is quasi-continuous. It is also clear from the figure that these energies occur at different wave vectors **Q**, and that the wave vector is different in both magnitude and direction as the time-of-arrival changes. Therefore the time-of-flight spectrometer is generally better suited for investigating the dynamics of systems where the excitations depend only on the magnitude of **Q**, and not its direction. Each detector then can be thought of as sweeping out a trajectory in (Q, E) as shown on the right-hand side of Fig. 10. Examples of systems that are well matched to the time-of-flight capability are structurally randomized systems such as glasses, liquids, or measuring density-of-states in polycrystalline samples. It is also very useful in situations when one wants to study the energetics of "isolated" particles or ions, where the excitations are dispersionless, such as in the case of low concentrations of impurities, diffusion, tunneling, for many molecular vibrations, or magnetic crystal field levels. This contrasts with triple-axis spectrometry, whose strength is realized when investigating collective excitations of materials such as lattice vibrations (phonons), excitons, and spin waves (magnons), particularly in single crystal specimens.

The disk chopper spectrometer uses several rotating disks to produce a monochromatic beam, in short bursts. The incident energy can be tuned continuously from ~1 meV to 20 meV, but is optimized for cold neutrons since it is on a cold-neutron guide. For energy-loss scattering the energy resolution is quite good as is characteristic of cold neutron instrumentation. For energy-gain processes, on the other hand, data can be obtained to quite high energy transfers, depending on the sample temperature. This mode of operation is opposite to the filter analyzer instrument, which uses high incident neutron energies, but cold final energies.

Fermi Chopper Spectrometer (FCS)

The Fermi Chopper Spectrometer is a time-of-flight instrument that uses a pair of pyrolytic graphite crystals to monochromate the incident beam, and then a chopper to create bursts of neutrons to enable the time-of-flight process. The incident energies can be selected between 2.2 and 15 meV, and there are ~100 detectors. The basic operation of the instrument is then the same as for the DCS instrument.

IV. Summary

The five types of instruments discussed allow measurements over a wide range of energies and a wide range of wave vectors. Figure 11 provides a summary and comparison of the capabilities of the Filter Analyzer Neutron Spectrometer (FANS), the Disk Chopper Spectrometer (DCS), the High Flux Backscattering Spectrometer (HFBS), and the Spin Echo Spectrometer. The triple

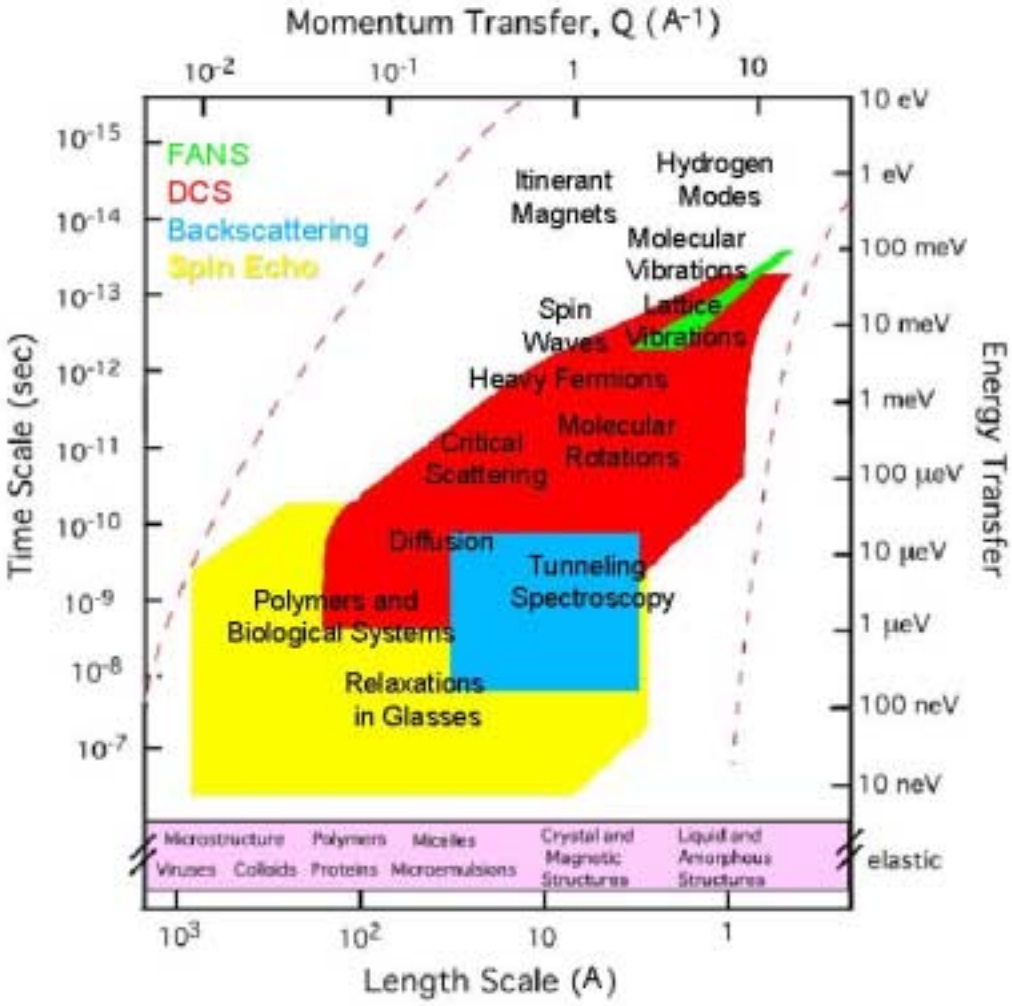

Fig. 11. Q, E diagram indicating the range of each of the spectrometers, and regions where various phenomena are typically found.

axis spectrometers and FCS have a similar (**Q**,E) to DCS. With the hands-on experience that you will have during the workshop, we hope that you will a develop an intuition for the types of measurements for which each instrument is optimized.